Second Half-Reaction of Nitric Oxide Synthase: Computational Insights into the Initial Step and Key Proposed Intermediate

Kyung-Bin Cho and James W. Gauld*

Department of Chemistry and Biochemistry, University of Windsor, Windsor, Ontario, N9B 3P4, Canada

Received: August 28, 2005; In Final Form: October 6, 2005

Density functional theory methods have been employed to investigate possible first steps in the second half-reaction of the mechanism of nitric oxide synthases (NOSs). In particular, reactions and complexes formed via transfer of either *or* both hydrogens of the substrates (NHA) −NHOH group to the Fe-bound O_2 were considered. For each of these pathways, the effect of adding an extra electron from tetrahydrobiotperin (H_4B) was also examined. The preferred initial pathway involves the simultaneous transfer of both hydrogens of the −NHOH group to the $Fe_{heme}-O_2$, without an additional electron, to give the $Fe_{heme}-HOOH$ species which lies only marginally higher in energy, 2.5 kcal mol^{-1} or less, than the initial bound active site. An alternative mechanism in which only the −NH− proton of the −NHOH group is transferred to the $Fe_{heme}-O_2$ to give an $Fe_{heme}-OOH$ derivative is found to require only slightly more energy, approximately 2 kcal mol^{-1}. However, transfer of the proton back to the −NOH nitrogen occurs without a barrier at 298.15 K. Tetrahedral intermediates in which the $Fe_{heme}-O_2$ has attached at the guanidinium carbon (C_{guan}) of NHA, that is, forms an $Fe_{heme}-O_2-C_{guan}$ link, have also been investigated. All examples of such species considered, that is, with or without hydrogen or electron transfers, lie significantly higher in energy by at least 29.0 kcal mol^{-1} than the initial bound active site. Thus, it is suggested that such complexes are not mechanistically feasible. The implications of the present findings for the second half-reaction are also discussed.

1. Introduction

Nitric oxide (NO) is an important biosignaling agent that has been found to play central roles in a diverse array of physiological processes within the cardiovascular, neuronal, and immunological systems.[1−3] In addition, it is also thought to play a role in various pathological diseases including cancer and Alzheimers.[4,5] Enzymatically, within the mammalian body, NO is produced by the class of enzymes known as nitric oxide synthases (NOSs).[6−8] While three isoforms are known within humans, neuronal (n), inducible (i), and endothelial (e) NOS, they have been found to possess similar active sites[9−12] and are thought to employ similar catalytic mechanisms. Recently, analogous enzymes have also been found in bacteria,[13] further enhancing interest in the enzymatic production of NO.

The overall mechanism of NOS occurs via the two half-reactions shown in Scheme 1. In the first, L-arginine undergoes two-electron oxidation with consumption of an O_2 to give N^{ω}-hydroxy-L-arginine (NHA). This is thought to occur via a mechanism similar to that of cytochrome P450-type enzymes.[14−16] The second half-reaction involves the further one-electron oxidation of NHA to L-citrulline and NO with consumption of a second O_2 molecule. However, unlike the first half-reaction, no analogous enzymatic mechanism is known. Consequently, the second half-reaction has been the subject of a number of investigations (see, for example, refs 9 and 17−22). Unfortunately, however, its exact mechanism remains unclear.

A number of mechanisms have, however, been proposed for the second half-reaction.[18,22] These various proposals exhibit some common key features, summarized in Scheme 2. We note that, in Scheme 2, the initial NHA substrate is shown in its protonated form as suggested by several recent experimental

SCHEME 1. Schematic Illustration of the Overall Mechanism of NOS

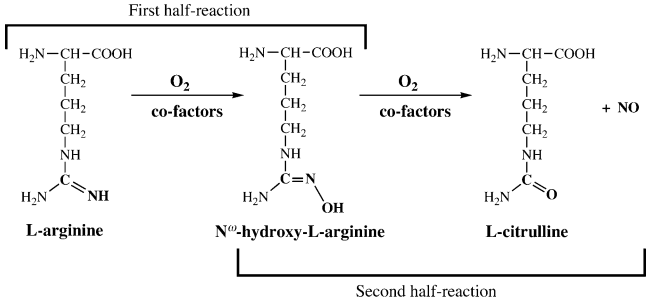

SCHEME 2: Summary of the Common Features of the Proposed Mechanisms for the Second Half-reaction: Initial Formation of (a) an $Fe_{Heme}-O_2$ Species, Subsequent Formation of (b) a Tetrahedral "Intermediate", and Formation of (c) the Final Products[a]

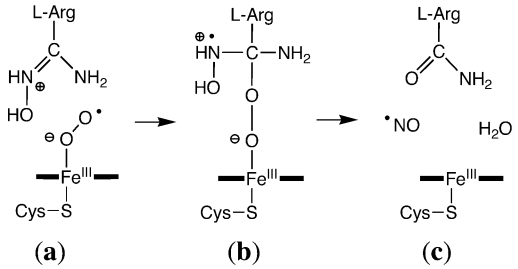

[a] Protonation and ionization states may vary. L-Arg denotes the part of L-arginine that is not altered during the reaction.

* To whom correspondence should be addressed. E-mail: gauld@uwindsor.ca.

10.1021/jp054864o CCC: $30.25
Published on Web 11/15/2005

and theoretical investigations.[19,20,23] It is generally accepted that, once NHA is generated via the first half-reaction, an O_2 molecule binds at the Fe_{heme} center of the active site. The resulting $Fe_{heme}-O_2$ species, or a derivative thereof, eventually goes on to attack at the guanidinium center (C_{guan}) of NHA to form an $Fe_{heme}-O-O-C_{guan}$ linked tetrahedral "intermediate", which ultimately goes on to give the products, L-citrulline and NO.

Despite these similarities, the proposed mechanisms differ significantly in key details, in particular, the crucial first step of the reaction. For example, several proposals have suggested that the second half-reaction is initiated by the transfer of the −NH− or −OH proton or hydrogen from the −NHOH group of NHA to the $Fe_{heme}-O_2$ moiety, thus forming a hydroperoxy-type species (for recent reviews, see refs 18 and 22). Alternatively, it has been proposed that the initial $Fe_{heme}-O_2$ moiety simply attacks the C_{guan} center of NHA to directly form the tetrahedral intermediate. In addition, it has also been suggested that the $Fe_{heme}-O_2$ may instead abstract an electron from NHA. More recently, however, it has been proposed[21] that the reaction begins with the addition of an electron to $Fe_{heme}-O_2$ from a tetrahydrobiopterin (H_4B) that binds adjacent to the active site. Indeed, there is experimental evidence suggesting that a pterin radical is formed transiently in the first half-reaction[24−26] and possibly, though with a markedly shorter lifetime, in the second half-reaction.[21] As a consequence of these differences, a variety of tetrahedral $Fe_{heme}-O_2-C_{guan}$ "intermediates", a common key structure in essentially all proposed mechanisms, have been proposed. However, the exact nature and feasibility of such intermediates remains unclear. Due to the importance of this class of enzymes and the novel insights into catalysis they provide, our current understanding of the mechanism of the second half-reaction is unsatisfactory.

Computational chemistry can act as a complementary tool to traditional experimental investigations. It can provide insights not only into the nature and feasibility of important mechanistic species but also into that of individual reaction steps within the overall mechanism. We have performed a detailed and comprehensive density functional theory (DFT)-based investigation on the key initial step of the second half-reaction of NOS. In particular, hydrogen and proton transfers and the effects of an addition of an electron from an external source such as H_4B, and their mechanistic implications, have been considered. In addition, to provide further insights, we have also investigated the nature and feasibility of a range of proposed and alternative $Fe_{heme}-O_2-C_{guan}$ tetrahedral intermediates.

2. Computational Methods

All DFT[27,28] calculations were performed employing the B3LYP[29−32] method as implemented in Gaussian 03[33] (transition structure optimizations and frequencies) and Jaguar 5.5[34] (all other calculations). For geometry optimizations and frequency calculations, the LACVP basis set was used on all atoms except sulfur, for which the LACV3P** basis set was used. Solvent effects were calculated by performing single-point calculations at this same level of theory using Jaguar's Poisson−Boltzmann solver with a dielectric constant of 4.0. Relative energies and spin density values were obtained by performing single-point calculations using the larger LACV3P** basis set on the above optimized geometries. Relative free energies at 298.15 K were calculated by including the appropriate zero-point vibrational energy, solvation, thermal enthalpy, and entropy corrections. All energies mentioned in the discussion are relative free energies. Similar computational method models have been previously employed to investigate related enzymatic systems. The applicability of such methods for the study of such systems is discussed further within refs 35−38.

TABLE 1: Relative Energies (kcal mol^{-1}) for Various Multiplicities of the Active Site with NHA and O_2 Bound

multiplicity	relative energy[a]	solvent correction	frequency correction[b]	relative free energy[c]
1[d]	0.0	+0.0	+0.0	0.0
1[e]	3.6	−2.1	−0.1	1.4
3[d]	9.1	+0.3	−2.6	6.9
5[d]	7.9	−0.3	−2.1	5.5
7[d]	7.5	−0.3	−5.5	1.7
9[d]	42.6	+0.6	−4.9	38.2

[a] Large basis set single-point energy (see text). [b] Combined zero-point vibrational energy, thermal enthalpy, and entropy contributions at 298.15 K. [c] Relative free energy = relative energy + solvent + frequency. [d] Binding as in Figure 1a. [e] Binding as in Figure 1b.

The active site models used include an Fe-porphyrin for heme, thiolmethyl anion for Cys194 (iNOS numbering), acetate for Glu371, and 1-methyl-2-hydroxy-guanidinium for NHA, that is, the substrate is considered protonated as previously suggested.[19,20,23] The backbone chain between the carboxylate carbon of Asn364 and the amide of Tyr367 was also included. The total charge of the model was −1, with the initial iron oxidation state set as [Porphyrin−Fe(III)−OO]$^{0+}$. When modeling the effects of addition of an electron, the total charge was set to −2. To mimic protein constraints during optimization, five atoms (marked by X in the figures) were held fixed in their corresponding crystal structure positions (PDB: 1DWX[9]). Similar approaches have been previously employed for enzymatic systems, including NOS, and found to provide reasonable estimates for obtaining, for example, relative free energies.[35−39]

For calculation of the ionization potential of H_4B, it was placed in a model of its iNOS binding site[9] which included appropriate models of the amino acids and groups with which it directly interacts: Ser112, Arg375, Trp457, Ile456, Leu458, and one of the heme propionate arms. As above, relevant cutoff atoms corresponding to the protein backbone or the porphyrin ring were held fixed. The total net charge of the model, before ionization, was set to 0.

3. Results and Discussion

Initial Structure of the Active Site with NHA + O_2 Bound. The binding of O_2 and NHA within the active site has been previously considered.[23] Herein, we have further examined such complexes and obtained their relative free energies, listed in Table 1. A detailed breakdown of the energies is given in Table S1. The singlet state of the bound active site is found to be preferred, lying slightly lower in energy than the heptet state by 1.7 kcal mol^{-1}. Similar to that previously observed,[23] two modes of interaction between $Fe_{heme}-O_2$ and NHA are found for the singlet state (Figure 1). In the preferred binding mode, **1a**, the −NH− and −OH of the −NHOH group of NHA form two moderately short hydrogen bonds (1.94 and 1.61 Å) to the outer and inner oxygens of $Fe_{heme}-O_{in}-O_{out}$, respectively (Figure 1a). The alternative binding mode in which the hydrogen bonds are interchanged, **1b**, lies just 1.4 kcal mol^{-1} higher in energy (Figure 1b). Unlike **1a**, however, one hydrogen bond is quite short ($OH\cdots O_{out}$, 1.52 Å) while the other is dramatically longer ($NH\cdots O_{in}$, 2.88 Å). In both **1a** and **1b**, the O−O bond maintains considerable multibond character (1.38 Å). The alternative states 3, 5, and in particular 9, although structurally similar (Table S2), all lie distinctly higher in energy than either 1 or 7 (see Table 1).

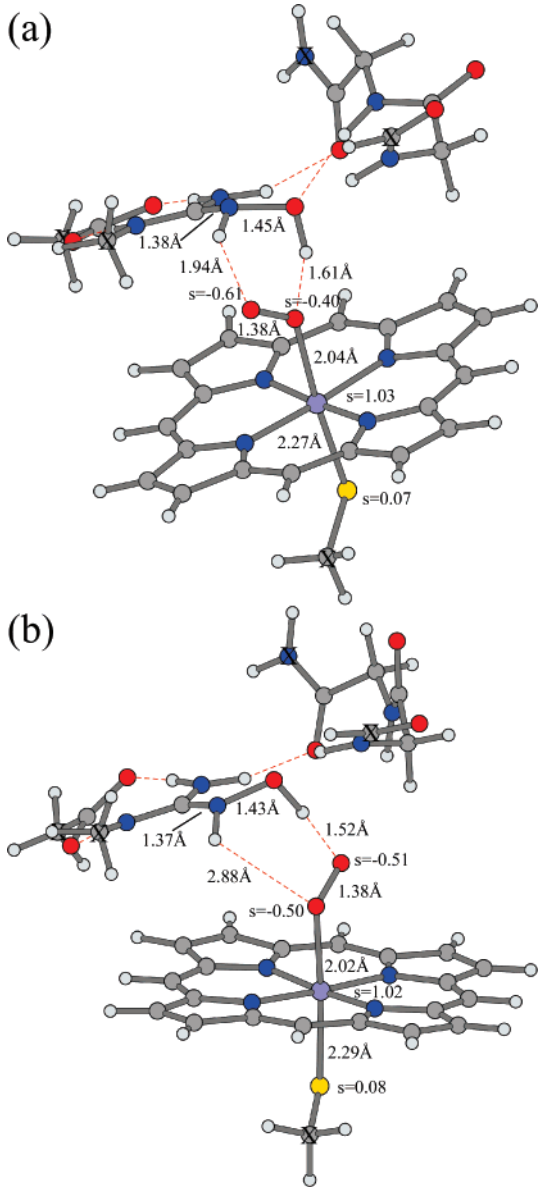

Figure 1. Optimized structures and spin distributions of the (a) preferred and (b) alternative conformers of the active site with NHA and O_2 bound, multiplicity = 1 (see text; red = O, blue = N, yellow = S, gray = C, and purple = Fe; X denotes atoms held fixed during optimization).

Transfer of a Single H•/H$^+$ from NHA to Fe$_{heme}$−O$_2$. It has been proposed[18,22] that the initial step involves the transfer of a single H• or H$^+$ from the −NHOH group of NHA to Fe$_{heme}$−O$_2$ to form a hydroperoxo species. Indeed, the organization of the preferred initial bound active site **1a** suggests such a possibility, in particular, transfer of the −NH− or −OH hydrogen to the outer or inner Fe$_{heme}$−O$_{in}$−O$_{out}$ oxygen, respectively.

However, for any appropriate multiplicity (1, 3, 5, 7), no stable structures were located corresponding to transfer of the −OH hydrogen to O$_{in}$. In contrast, optimized structures for the transfer of the −NH− proton to O$_{out}$ were obtained at multiplicities 1, 5, and 7 with relative free energies, with respect to **1a**, of 15.9, 15.1, and 13.5 kcal mol^{-1}, respectively. The optimized structure of the singlet state (**2^1**), the same state as **1a**, is shown in Figure 2. Similar to **1a**, there are two moderately short hydrogen bonds between the resulting −NOH of the substrate and HOO−Fe$_{heme}$ group: r(N···HO$_{out}$) = 1.70 Å and r(OH···O$_{in}$) = 1.73 Å. In addition, the O$_{out}$−O$_{in}$ bond (1.50 Å)

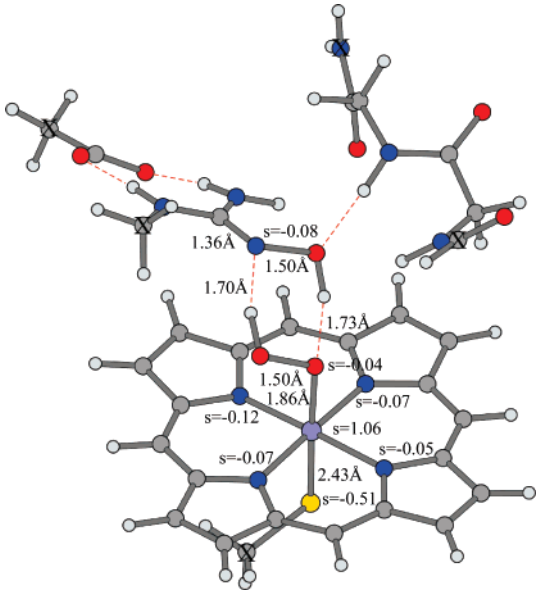

Figure 2. Optimized structure and spin distribution of the hydroperoxy species resulting from the proton transfer from the −NH− moiety of NHA to O$_{out}$, multiplicity = 1 (see text; red = O, blue = N, yellow = S, gray = C, and purple = Fe; X denotes atoms held fixed during optimization).

has lengthened such that it is now essentially an O−O single bond. We note that the structures of the 5 and 7 states are similar, exhibiting the same general features, for example, hydrogen bond arrangement (Table S2).

However, the hydroperoxy species are not very stable. For any multiplicity, back-donation of the proton from the HOO− moiety to the nitrogen center of the substrate −NOH group occurs with little or no barrier. For example, for **2^1**, the calculated barrier for the above proton transfer is 13.0 kcal mol^{-1} relative to **1a** (data not shown). Experimentally, no signal due to the formation of a hydroperoxy species such as **2** has been observed.[40] It was suggested that this may be due either to the lack of formation or to the nonaccumulation of such a species. The present results of only transient formation of any Fe$_{heme}$−OOH species, at best, appear to support these conclusions.

Double Transfer of H•/H$^+$ from NHA to Fe$_{heme}$−O$_2$. While it has not been proposed as a possible first step of the second half-reaction of NOS, the optimized structure of **1a** suggests that it may be possible to transfer both hydrogens from the −NHOH fragment of NHA to the Fe$_{heme}$−O$_2$ group. In particular, it suggests that the −NH− proton and −OH hydrogen may be able to transfer cooperatively to O$_{out}$ and O$_{in}$, respectively, thus forming an Fe$_{heme}$-bound HOOH species.

Indeed, for all multiplicities 1 (**3^1**), 3 (**3^3**), 5 (**3^5**), and 7 (**3^7**) considered, optimized structures of such a species were obtained with relative free energies just 2.5, 1.9, 2.3, and 1.6 kcal mol^{-1} higher than **1a**, respectively. Due to the fact that it is the same state as **1a**, thus representing the direct corresponding product, the optimized structure of **3^1** is shown in Figure 3. There are two moderately short hydrogen bonds between the resulting −NO and HOOH− group: r(N···HO$_{out}$) = 1.71 Å and r(O··· ·HO$_{in}$) = 1.94 Å. In addition, the O$_{out}$−O$_{in}$ bond has also lengthened considerably to 1.52 Å. Structurally, as noted for the initial active sites and hydroperoxy species, the various multiplicities all exhibit the same general features (Table S2).

As observed for the hydroperoxy species **2**, the heptet state lies slightly lower in energy (0.9 kcal mol^{-1}) than the singlet. Indeed, while the singlet Fe$_{heme}$−HOOH species is calculated to lie slightly higher in energy than **1a**, the corresponding heptet

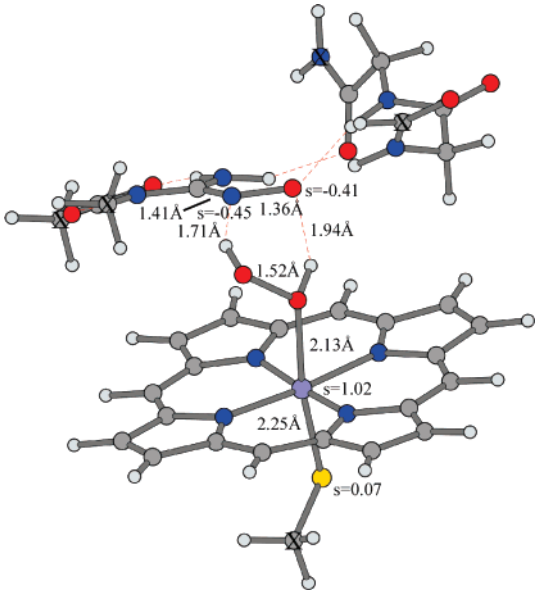

Figure 3. Optimized structure and spin distribution of the $Fe_{heme}-HOOH$ species resulting from the transfer of both hydrogens of the $-NHOH$ group to $Fe_{heme}-O_2$, multiplicity = 1 (see text; red = O, blue = N, yellow = S, gray = C, and purple = Fe; X denotes atoms held fixed during optimization).

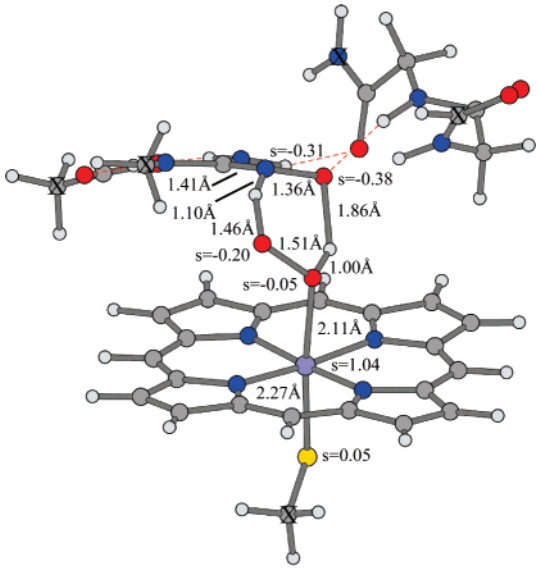

Figure 4. Optimized structure and spin distribution of the transition structure for the formation of the $Fe_{heme}-HOOH$ species from **1a**, multiplicity = 1 (see text; red = O, blue = N, yellow = S, gray = C, and purple = Fe; X denotes atoms held fixed during optimization).

is calculated to be essentially thermoneutral with the heptet state of the initial bound active site (cf. Table 1). It should be noted, however, that these small energy differences lie within expected error margins.

To further elucidate the feasibility of the formation of such species, the transition structures (TS) for the formation of $\mathbf{3^1}$ and $\mathbf{3^7}$ from the appropriate state initial bound active sites were located. They were found to lie 14.6 (**TS 4^1**) and 12.1 (**TS 4^7**) kcal mol^{-1}, respectively, higher in energy than **1a**. Importantly, the energy required for the formation of the $Fe_{heme}-HOOH$ species in either state (1 or 7) is marginally lower than that required to form the hydroperoxy species $\mathbf{2^1}$ or $\mathbf{2^7}$ and, furthermore, leads to the formation of considerably more stable product complexes.

The optimized structure for **TS 4^1** is shown in Figure 4. Again the structures of the singlet and heptet are quite similar (Table S2). As illustrated by **TS 4^1**, the $-NHO-H$ distance (1.86 Å) has lengthened considerably such that the hydrogen can be considered to be almost wholly transferred to O_{in}. Concomitantly, the $-N(-H)OH$ distance has also lengthened significantly by approximately 0.07 Å to 1.10 Å. Thus, it is already partially transferred to O_{out}. We note that we have performed a detailed scan of the heptet surface for the $H^{\bullet}/H^{+}$ transfer from $-NHOH$ to the $-O_2$ moiety (Figure S1). The results also indicate that simultaneous transfer of both hydrogens is preferred to transfer of either one alone.

Experimentally, H_2O_2 has been observed to be able to support the second half-reaction of NOS.[41] The above findings suggest that it may in fact be able to bind to the Fe_{heme} center, forming an initial intermediate-like complex. We note that in P450−,[15] and in particular, peroxidase-type enzymes,[42−44] related heme-bound oxygen derivatives can react to form activated derivatives, for example, compound I, via release of O_{out} as H_2O. It has been suggested that the $-OH$ hydrogen of NHA "is not relevant" to the mechanism of NOS.[18] We note that the formation of **2** requires only slightly more energy than for the formation of **3**. Thus, if the $-OH$ hydrogen is "missing" or replaced by an alkyl substituent, to form a compound I-like derivative without the NHA $-OH$ hydrogen, then one could possibly transfer just the

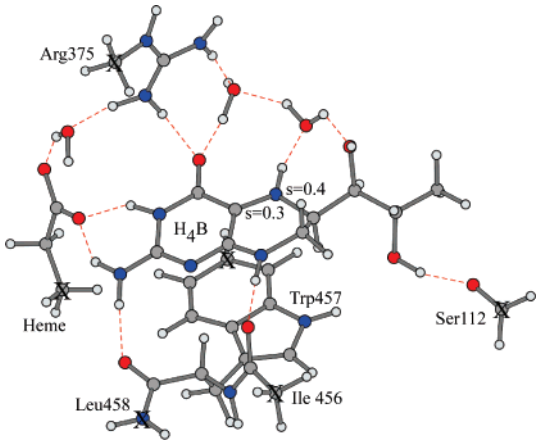

Figure 5. Binding and selected spin distribution of $H_4B^{\bullet+}$ within its NOS binding site[9] (see text; red = O, blue = N, and gray = C; X denotes atoms held fixed during optimization).

$-NH-$ proton to O_{out} while obtaining a H^+ or $H^{\bullet}$ from an alternate source. This is analogous to that proposed to occur in the first half-reaction of NOS. Hence, the $-OH$ hydrogen may simply be *nonessential*, that is, the above results do not exclude the possibility of reaction paths proceeding via **2**.

Addition of an Electron from H_4B. In several proposed mechanisms,[18,22] it has been suggested that the binding of O_2 to the Fe_{heme} center occurs with the addition of an electron from a cofactor of NOS. Recently, it has been suggested that a H_4B adjacent to the active site transiently donates this electron.[21]

To consider the thermochemistry of complexes involving the addition of an electron from H_4B, one needs to take into account the ionization energy of bound H_4B. The arrangement and preferred selected spin distribution of $H_4B^{\bullet+}$ within the binding site model employed is shown in Figure 5. The ionization energy of bound H_4B was calculated to be 101.9 kcal mol^{-1}. In addition, one can also estimate the change in the Coulombic interaction energy ($q_1q_2/\epsilon r^2$) between the heme and H_4B sites upon electron transfer; the parameters used for the sites after electron transfer were a charge of −2 on the heme (centered on Fe) and +1 for the H_4B site (centered on the preferred site of ionization), an approximate charge center separation distance of 15 Å, all within

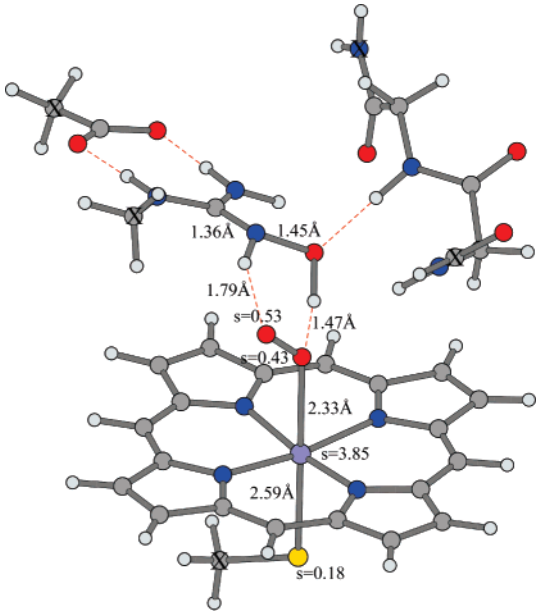

Figure 6. Optimized structure and selected spin distribution of the peroxy anion derivative formed upon the addition of an electron to the NOS active site **1a**, multiplicity = 6 (see text; red = O, blue = N, yellow = S, gray = C, and purple = Fe; X denotes atoms held fixed during optimization).

an environment of $\epsilon = 4$. The resulting change in the interaction energy is 11.1 kcal mol^{-1} *in favor* of electron transfer. Hence, the energy required to transfer an electron from bound H_4B to the heme is approximately 90.8 kcal mol^{-1}. This "electron-transfer energy" has been included where appropriate in the relative free energies discussed below. We note that a similar approach has been used previously[45] to approximate the energy of such changes in related enzyme systems.

Potentially, the addition of an electron to the $Fe_{heme}-O_2$ moiety could occur with or without $H^+/H^\bullet$ transfer from the −NHOH group of NHA. Hence, we have considered the structures and relative energies of possible complexes formed via both approaches.

Addition of an Electron from H_4B, without $H^+/H^\bullet$ Transfer. An electron was added to **1a** and then reoptimized for a range of possible multiplicities, 2, 4, and 6. However, only multiplicity = 6 gave an Fe_{heme}-bound peroxy anion derivative (**6**^{6}), the others either dissociated or optimized to alternative complexes (see below). The optimized structure and selected spin distribution are shown in Figure 6. It can be clearly seen that the preferred hydrogen bonding arrangement between −NHOH and $Fe_{heme}-O_2$ is maintained, although understandably the interactions are much shorter than in **1a** by 0.14−0.15 Å (cf. Figure 1a). Complex **6**^{6} lies 62.6 kcal mol^{-1} lower in energy than the initial active site **1a**, which is due in large part to the greater interaction with the surrounding environment upon increasing the negative charge (see Table S1). However, the inclusion of the energy required to transfer an electron from H_4B results in **6**^{6} in fact lying higher in energy than **1a** by 28.3 kcal mol^{-1}. This is significantly higher by at least 12 kcal mol^{-1} than that required for the formation of the $Fe_{heme}-OOH$ or $Fe_{heme}-HOOH$ derivatives (see above).

Addition of an Electron from H_4B, with $H^+/H^\bullet$ Transfer. As noted above, an alternative possibility is that the addition of an electron is in some manner coupled with proton or hydrogen transfer from the −NHOH group of NHA to the $Fe_{heme}-O_2$ moiety. Indeed, a considerable shortening of the hydrogen bonds involving the mechanistically important −NHOH

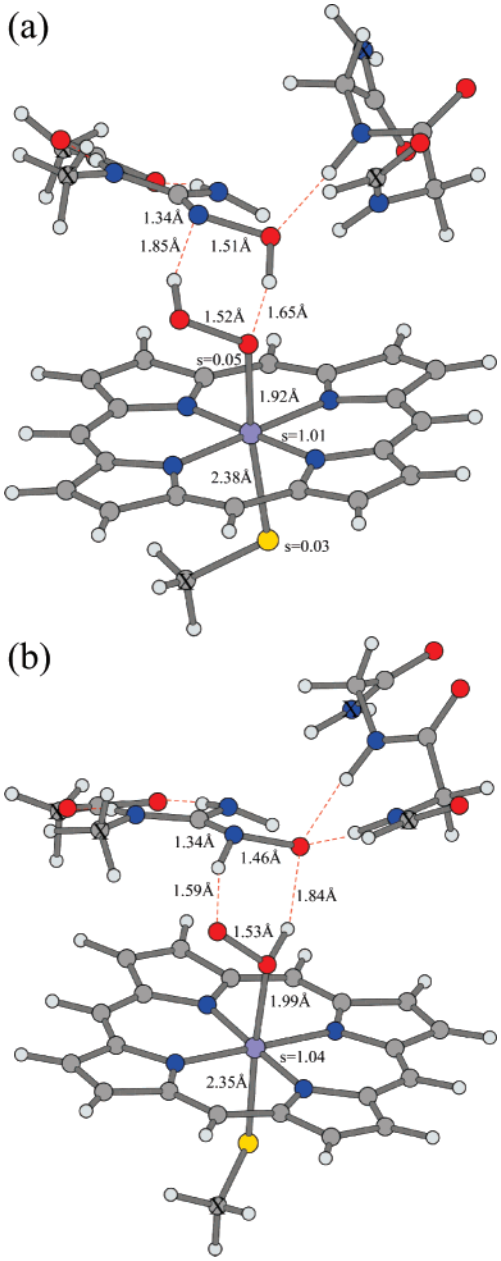

Figure 7. Optimized structure and spin distribution of the hydroperoxy complexes formed by the transfer of the (a) −NH− proton to O_{out} and (b) −OH hydrogen to O_{in} upon addition of an electron to the active site, multiplicity = 2 (see text; red = O, blue = N, yellow = S, gray = C, and purple = Fe; X denotes atoms held fixed during optimization).

hydrogens was noted for **6**^{6}. Hence, based on the hydrogen bonding arrangement between −NHOH and $Fe_{heme}-O_2$, we investigated complexes formed by the transfer of the −NH− proton and/or −OH hydrogen to O_{out} and O_{in}, respectively. In addition, we considered a range of possible appropriate multiplicities for such complexes 2, 4, and 6.

For the addition of an electron with the transfer of the −NH− proton to O_{out}, stable complexes were obtained for all multiplicities 2, 4, and 6. Their relative energies with respect to **1a**, with inclusion of the "electron-transfer energy" were 17.5, 49.6, and 19.5 kcal mol^{-1}, respectively. The optimized structure for the doublet state (**7**^{2}), the lowest energy complex, is shown in Figure 7a. As for the analogous $Fe_{heme}-OOH$ species (**2**), complex **7**^{2} has two relatively short hydrogen bonds between −NOH and −OOH, $r(N\cdots HO_{out}) = 1.85$ Å, $r(OH\cdots O_{in}) = 1.65$ Å, and the O−O bond has lengthened to 1.52 Å. While the quartet state is

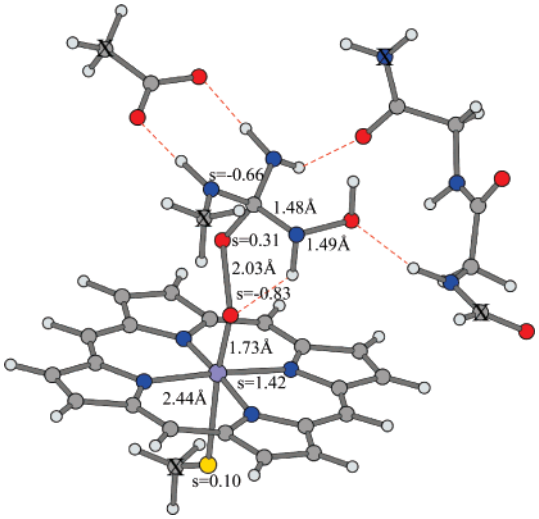

Figure 8. Optimized structure and selected spin distribution for the transition structure formed by the direct attack of the $Fe_{heme}-O_2$ moiety at C_{guan} of the substrate NHA, multiplicity = 1 (see text; red = O, blue = N, yellow = S, gray = C, and purple = Fe; X denotes atoms held fixed during optimization).

clearly too high in energy, both the doublet and sextet complexes lie only a few kcal mol^{-1} higher in energy than the complexes formed by proton transfer from −NH− *without* the addition of an electron. Thus, while they are relatively low in energy, the addition of an electron to generate such complexes is not energetically favorable. Furthermore, they also lie considerably higher in energy by approximately 16 kcal mol^{-1} than the Fe_{heme}−HOOH complexes formed without the addition of an electron.

For the addition of an electron with the transfer of the −OH hydrogen to O_{in}, stable complexes were also obtained for each multiplicity 2, 4, and 6. The optimized structure of the doublet state is shown in Figure 7b. In contrast, however, their relative energies with respect to **1a**, with inclusion of the "electron-transfer energy", were markedly higher, being 31.7, 35.1, and 35.1 kcal mol^{-1}, respectively.

Possible complexes arising from the addition of an electron *and* transfer of both −NHOH hydrogens to the Fe-bound O_2 moiety were also examined for a range of appropriate multiplicities, 2, 4, and 6 (not shown). However, they were all found to either result in the release of H_2O_2 from the Fe center or lie considerably too high in energy to be mechanistically relevant. We note that the fact that almost all possible initial complexes formed with inclusion of an extra electron from H_4B are too high in energy does not preclude H_4B from acting as an electron donor. Rather, it may occur at a later step in the reaction. Indeed, experimental studies have suggested that if such an electron transfer occurs, it occurs sometime after binding of O_2 to the Fe center but before NO formation and its binding to the Fe center.[21,46]

Investigations on Proposed Tetrahedral "Intermediates". A common feature of essentially all mechanisms proposed for the second half-reaction is the formation of an enzyme−substrate complex in which the $Fe_{heme}-O_2$ moiety attacks at the guanidinium carbon (C_{guan}) of NHA,[18,22] that is, forms an Fe_{heme}−O−O−C_{guan} linked complex (hereafter referred to as a tetrahedral intermediate). The exact nature of this intermediate depends on the initial step in the reaction. For example, it has been suggested that the formation of the tetrahedral intermediate requires either an initial hydrogen or electron transfer as considered above or a direct attack of the initial $Fe_{heme}-O_2$ group at the C_{guan} center. Thus, a greater understanding of such an intermediate can provide further insights into the various possible initial steps as well as the overall mechanism.

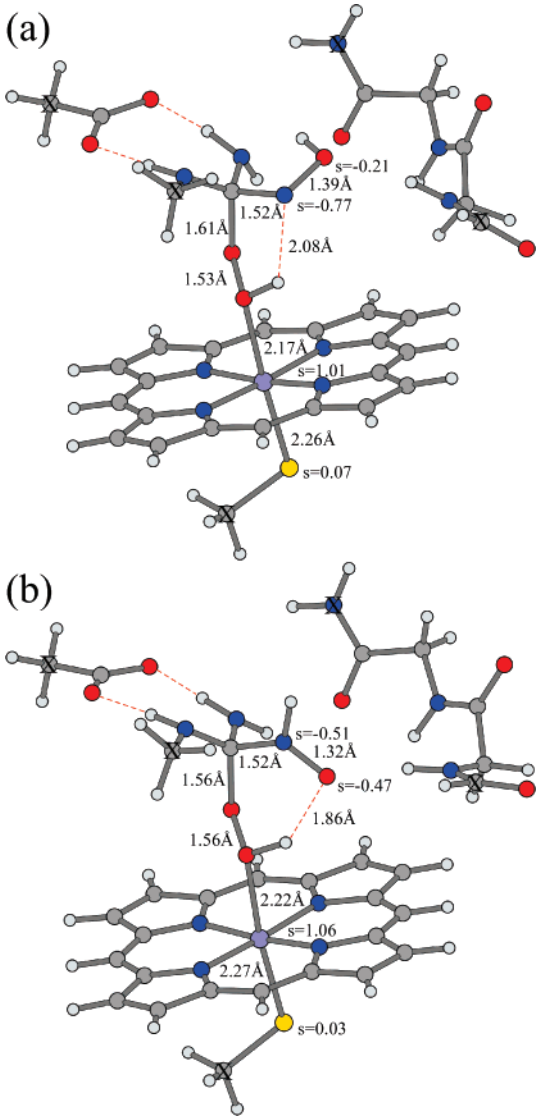

Figure 9. Optimized structure and selected spin distribution for tetrahedral intermediates formed with the transfer of the (a) −NH− proton or (b) −OH hydrogen to O_{in}, multiplicity = 1 (see text; red = O, blue = N, yellow = S, gray = C, and purple = Fe; X denotes atoms held fixed during optimization).

Direct Formation: No Electron or $H^+/H^\bullet$ Transfer. Direct attack of $Fe_{heme}-O_2$ at C_{guan} has been previously[23] found to not give a stable intermediate. However, it is possible that it is instead a transition structure along the reaction path. This was indeed found to be the case; the optimized structure for the singlet state (**TS 8**) is shown in Figure 8. As illustrated by the considerably lengthened (2.03 Å) $O_{out}-O_{in}$ bond, **TS 8** corresponds to the transfer of O_{out} from $Fe_{heme}-O_2$ to C_{guan} (cf. Figure 1). However, it lies approximately 66.6 kcal mol^{-1} higher in energy than **1a**. Thus, it is energetically unlikely that such a TS plays a role in the mechanism.

Formation Involving Transfer of $H^+/H^\bullet$ from −NHOH to $Fe_{heme}-O_2$. An alternative possibility is that the formation of a tetrahedral intermediate, without the addition of an electron, involves the transfer of either −NHOH hydrogen to the $Fe_{heme}-O_2$ group. Such stable complexes were indeed found for all multiplicities considered (1, 3, 5, and 7). The optimized structures for the singlet intermediates formed by the transfer

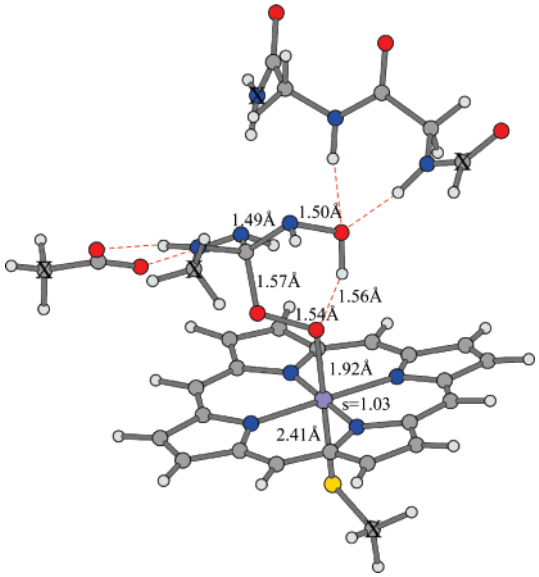

Figure 10. Optimized structure and selected spin distribution of the tetrahedral intermediate with the addition of an electron to **1a**, multiplicity = 2 (see text; red = O, blue = N, yellow = S, gray = C, and purple = Fe; X denotes atoms held fixed during optimization).

of the −NH− or −OH hydrogen, **9a**[1] and **9b**[1], respectively, are shown in Figure 9. As can be seen, the transfer of either hydrogen occurred to O_{in}. It is also interesting to note that complexes resulting from the transfer of the −NH− proton contain an $O_{in}H\cdots N_{NHA}$ hydrogen bond (2.08 Å), while those from the transfer of the −OH hydrogen contain an $O_{in}H\cdots O_{NHA}$ hydrogen bond (1.86 Å). The optimized structures for the other multiplicities exhibit the same general features and hydrogen bond interactions (Table S2).

The relative free energies, with respect to **1a**, of the tetrahedral intermediates formed via the transfer of the −NH− proton are 44.5, 42.9, 38.7, and 40.0 kcal mol^{-1} for multiplicities 1, 3, 5, and 7, respectively. In contrast, those involving the transfer of the −OH hydrogen lie lower in energy for all multiplicities at 30.2, 29.4, 29.0, and 29.2 kcal mol^{-1}, respectively. Hence, all such possible complexes lie significantly higher in energy in **1a**. In addition, it should be noted that these energies do not include the barrier heights for their formation which will further increase the energy required in order to mechanistically access such complexes. In general, enzymatic mechanisms occur with rate-limiting barriers of 20−25 kcal mol^{-1} or less. For NOS, experimental[8,47] kinetic data suggests, via the Eyring equation, an overall barrier for the second half-reaction of approximately 17 kcal mol^{-1}. Thus, such complexes are unlikely to play a role in the catalytic mechanism.

Intermediates with an Additional Electron from H_4B. Another possibility is that the formation of the tetrahedral intermediate occurs after the active site has gained an additional electron from H_4B.

SCHEME 3. Schematic Illustration of the Structures and Relative Free Energies (kcal mol^{-1}) of All Initial Complexes and Tetrahedral Intermediates Considered in This Present Study[a]

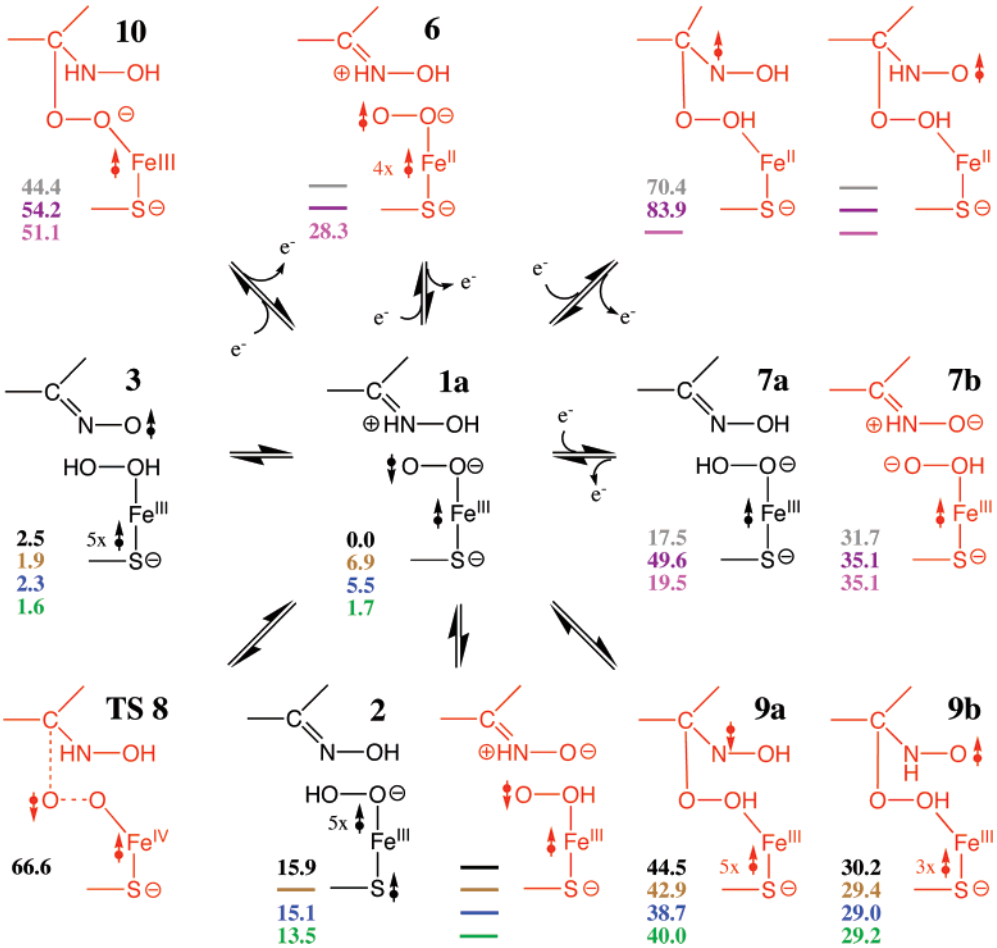

[a] Structures in red denote those too high in energy to be mechanistically feasible at any multiplicity. Schematic charge and radical distributions correspond to the lowest energy state, and numbering corresponds to the figures.

Initially, we considered such intermediates that did not also involve the transfer of either of the −NHOH hydrogens to the $Fe_{heme}-O_2$ moiety, that is, the $Fe_{heme}-O_2$ moiety has simply attached at C_{guan}, for a range of appropriate multiplicities, 2, 4, and 6. A stable complex was obtained at each; the optimized structure of multiplicity = 2 (**10²**) is shown in Figure 10. We note that the structures for the other multiplicities exhibit the same general features (Table S2). With the inclusion of the calculated "electron-transfer energy", these complexes are found to lie significantly higher in energy than **1a** by approximately 44.4, 54.2, and 51.1 kcal mol^{-1} for multiplicities 2, 4, and 6, respectively. Thus, such complexes lie at least as high in energy as the intermediates formed via transfer of either of the −NHOH hydrogens to O_{in} but without an additional electron (cf. Figure 9).

Possible tetrahedral intermediates were also considered that involve the addition of an electron *and* transfer of either −NHOH hydrogen to the $-O_2$ moiety, for a range of appropriate multiplicities (2, 4, and 6). Such intermediates can be thought of as (i) arising from the addition of an electron to **1a** followed by an attack of the resulting $Fe_{heme}-O_2$ moiety at C_{guan} with concomitant or sequential transfer of either the −NHOH hydrogen to the $-O_2$ moiety or simply (ii) the addition of an electron to those tetrahedral intermediates shown in Figure 9. For simplicity, we will refer to them as the latter. Stable complexes (not shown) corresponding to the addition of an electron to **9a**, that is, with transfer of the −NH− proton, were only obtained for multiplicities 2 and 4. However, with inclusion of the "electron-transfer energy", they are found to lie higher in energy than **1a** by 70.4 and 83.9 kcal mol^{-1} respectively! Thus, such structures are simply not enzymatically feasible. In contrast, no stable complexes corresponding to the addition of an electron to **9b**, that is, with the transfer of the −OH hydrogen, were obtained at any multiplicity (2, 4, or 6).

A schematic summary of the structures and relative free energies of all complexes and intermediates considered in this present study is provided in Scheme 3. As can be seen, all of the tetrahedral intermediates lie considerably higher in energy than any of the stable initial complexes obtained via transfer of either one or both −NHOH hydrogens to the $-O_2$ moiety, with or without an electron. We note that we also have performed calculations at the B3LYP/6-311+G(2df,p)//B3LYP/6-31G(d,p) + ZPVE level on a smaller model system in which we have compared the energy of the separated reactants, that is, the substrate ($CH_3NHC(NH_2)NHOH^+$/Arg−$NHOH^+$) + •OH/•OOH with that of the corresponding tetrahedral intermediate in which the •OH or •OOH are bound at the C_{guan} position. In addition, we have also performed the corresponding calculations using OH^- and OOH^-. Interestingly, both tetrahedral intermediates formed using •OH or OH^- are significantly lower in energy (by 123.9 and 44.0 kJ mol^{-1}, respectively) than when •OOH or OOH^- is employed, respectively (Table S3).

4. Conclusions

We have performed a detailed and comprehensive DFT-based investigation on proposed and alternative initial complexes and tetrahedral intermediates of the second half-reaction of NOS. For the initial bound active site, that is, NHA and O_2 bound, the singlet state is found to be preferred with the heptet slightly higher in free energy by 1.7 kcal mol^{-1}. Structurally, two relatively short hydrogen bonds are formed between the −NHOH group of NHA and the $Fe_{heme}-O_2$ moiety (**1a**), specifically, $-NH\cdots O_{out}$ and $-OH\cdots O_{in}$. We note that the initial active site is the only case in which the singlet was calculated to lie lower in energy than the heptet. However, for all appropriate structures except one (**9a**), these two states lie within 2.4 kcal mol^{-1} of each other.

Similar to that proposed, the lowest energy initial step is found to involve transfer of the −NHOH hydrogens to the $Fe_{heme}-O_2$ moiety. However, unlike those proposed, the lowest energy initial reaction step is found to involve the coordinated transfer of *both* −NHOH hydrogens to the $Fe_{heme}-O_2$ moiety, thus giving the corresponding Fe_{heme}−HOOH species (**3**). In particular, the −OH *and* −NH− hydrogens are transferred to O_{in} and O_{out}, respectively. The reaction barrier heights for the formation of Fe_{heme}−HOOH at multiplicities 1 and 7 were just 14.6 and 12.1 kcal mol^{-1}, respectively, with respect to **1a**. Singlet Fe_{heme}−HOOH was found to lie just 2.5 kcal mol^{-1} higher in energy than **1a** while for multiplicities 3, 5, and 7, such species were found to in fact lie slightly lower in energy than the corresponding bound active site state, by 0.1−5.0 kcal mol^{-1}. Significantly, the Fe_{heme}−HOOH species were found to be the lowest energy complexes, not including the initial bound active site, of all those considered.

An alternative pathway is found to involve the transfer of only the relevant −NH− hydrogen of NHA to O_{out} of the $Fe_{heme}-O_2$ moiety. Optimized structures of the resulting $-NOH\cdot\cdot\cdot HOO-Fe_{heme}$ complexes were obtained for multiplicities 1, 5, and 7 and were found to lie higher in energy than **1a** by 15.9, 15.1, and 13.5 kcal mol^{-1}, respectively. However, transfer of the hydrogen from Fe_{heme}−OOH back to the nitrogen center of the −NOH group occurs with little or no barrier. Thus, while the formation of such hydroperoxy species requires only slightly more energy (less than 2 kcal mol^{-1}) than for the formation of the alternative Fe_{heme}−HOOH derivatives, they are predicted to be notably less stable.

The addition of an electron from H_4B to either the initial active site or any of the intermediates formed by transfer of one or both of the −NHOH hydrogens was also considered. However, all resulting complexes, if stable, are found to lie too high in energy to be mechanistically relevant. An exception is those Fe_{heme}−OOH derivatives (**7a**) also formed with the transfer of the relevant −NH− proton of NHA to O_{out}. However, while they do lie within +20 kcal mol^{-1} of **1a** for multiplicities 2 and 6, they are still 1.6−6.0 kcal mol^{-1} higher in energy than the corresponding Fe_{heme}−OOH species formed *without* an additional electron. Hence, they do not represent a thermodynamically preferred complex for obtaining an extra electron from H_4B.

All complexes considered formed via the sole transfer of the −OH hydrogen of NHA to O_{in}, with or without an additional electron, were found to lie too high in energy to be mechanistically feasible or were not stable.

In addition to the investigation on possible first steps in the mechanism of the second half-reaction of NOS, a variety of proposed and alternative tetrahedral intermediates was also considered. These species all involve the attack of an $Fe_{heme}-O_2$ species, at the guanidinium carbon (C_{guan}) of NHA either directly or with the transfer of a hydrogen of the −NHOH group, all with and without an electron from H_4B. However, all such $Fe_{heme}-O_2-C_{guan}$-type complexes were found to either not be stable or lie significantly too high in energy to be mechanistically relevant. The lowest energy tetrahedral intermediate derivative examined, which also involves transfer of the −OH hydrogen of NHA to O_{in} (multiplicity = 5, **9b⁵**), is calculated to lie 29.0 kcal mol^{-1} higher in energy than **1a**.

A detailed and comprehensive investigation of the complete mechanism of the second half-reaction of NOS is currently in progress.

Acknowledgment. The authors are grateful to the Natural Sciences and Engineering Research Council of Canada (NSERC), Canadian Foundation for Innovation (CFI), and Ontario Innovation Trust (OIT) for financial support.

Supporting Information Available: The complete citation for ref 33, tables detailing the total energies and appropriate energy corrections, solvation, zero-point vibrational energy, enthalpy and entropy contributions at 298.15 K (Table S1), optimized structures in *xyz* format (Table S2), calculated total and relative energies for small chemical model systems (Table S3), and a schematic PES scan of the heptet surface for formation of the Fe_{heme}−HOOH species (Figure S1) are supplied. This material is available free of charge via the Internet at http://pubs.acs.org.

References and Notes

(1) Garthwaite, J.; Boulton, C. L. *Annu. Rev. Physiol.* **1995**, *57*, 683−706.

(2) Kerwin, J. F. J.; Lancaster, J. R. J.; Feldman, P. L. *J. Med. Chem.* **1995**, *38*, 4343−4362.

(3) MacMicking, J.; Xie, Q. W.; Nathan, C. *Annu. Rev. Immunol.* **1997**, *15*, 323−350.

(4) Ekmekcioglu, S.; Tang, C. H.; Grimm, E. A. *Curr. Cancer Drug Targets* **2005**, *5*, 103−115.

(5) Togo, T.; Katsuse, O.; Iseki, E. *Neurol. Res.* **2004**, *26*, 563−566.

(6) Marletta, M. A. *J. Biol. Chem.* **1993**, *268*, 12231−12234.

(7) Stuehr, D. J. *Biochim. Biophys. Acta* **1999**, *1411*, 217−230.

(8) Stuehr, D. J.; Griffith, O. W. In *Advances in Enzymology and Related Areas of Molecular Biology*; Meister, A., Ed.; Interscience: New York, 1992; Vol. 65, pp 287−346.

(9) Crane, B. R.; Arvai, A. S.; Ghosh, S.; Getzoff, E. D.; Stuehr, D. J.; Tainer, J. A. *Biochemistry* **2000**, *39*, 4608−4621.

(10) Crane, B. R.; Arvai, A. S.; Ghosh, D. K.; Wu, C.; Getzoff, E. D.; Stuehr, D. J.; Tainer, J. A. *Science* **1998**, *279*, 2121−2126.

(11) Fischmann, T. O.; Hruza, A.; Niu, X. D.; Fossetta, J. D.; Lunn, C. A.; Dolphin, E.; Prongay, A. J.; Reichert, P. R.; Lundell, D. J.; Narula, S. K.; Weber, P. C. *Nat. Struct. Biol.* **1999**, *6*, 233−242.

(12) Raman, C. S.; Li, H.; Martasek, P.; Kral, V.; Masters, B. S. S.; Poulos, T. L. *Cell* **1998**, *95*, 939−950.

(13) Adak, S.; Aulak, K. S.; Stuehr, D. J. *J. Biol. Chem.* **2002**, *277*, 16167−16171.

(14) Sono, M.; Roach, M. P.; Coulter, E. D.; Dawson, J. H. *Chem. Rev.* **1996**, *96*, 2841−2887.

(15) Shaik, S.; Kumar, D.; de Visser, S. P.; Altun, A.; Thiel, W. *Chem. Rev.* **2005**, *105*, 2279−2328.

(16) Denisov, I. G.; Makris, T. M.; Sligar, S. G.; Schlichting, I. *Chem. Rev.* **2005**, *105*, 2253−2277.

(17) Stuehr, D. J.; Santolini, J.; Wang, Z.-Q.; Wei, C.-C.; Adak, S. *J. Biol. Chem*. **2004**, *279*, 36167−36170.

(18) Huang, H.; Hah, J.-M.; Silverman, R. B. *J. Am. Chem. Soc.* **2001**, *123*, 2674−2676 and references therein.

(19) Tantillo, D. J.; Fukuto, J. M.; Hoffman, B. M.; Silverman, R. B.; Houk, K. N. *J. Am. Chem. Soc.* **2000**, *122*, 536−537.

(20) Tierney, D. L.; Huang, H.; Martasek, P.; Masters, B. S. S.; Silverman, R. B.; Hoffman, B. M. *Biochemistry* **1999**, *38*, 3704−3710.

(21) Wei, C. C.; Wang, Z. Q.; Hemann, C.; Hille, R.; Stuehr, D. J. *J. Biol. Chem.* **2003**, *278*, 46668−46673.

(22) Rosen, G. M.; Tsai, P.; Pou, S. *Chem. Rev.* **2002**, *102*, 1191−1199 and references therein.

(23) Cho, K. B.; Gauld, J. W. *J. Am. Chem. Soc.* **2004**, *126*, 10267−10270.

(24) Hurshman, A. R.; Krebs, C.; Edmondson, D. E.; Huynh, B. H.; Marletta, M. A. *Biochemistry* **1999**, *38*, 15689−15696.

(25) Wei, C. C.; Wang, Z. Q.; Arvai, A. S.; Hemann, C.; Hille, R.; Getzoff, E. D.; Stuehr, D. J. *Biochemistry* **2003**, *42*, 1969−1977.

(26) Wei, C. C.; Wang, Z. Q.; Wang, Q.; Meade, A. L.; Hemann, C.; Hille, R.; Stuehr, D. J. *J. Biol. Chem.* **2001**, *276*, 315−319.

(27) Kohn, W.; Sham, L. J. *Phys. Rev. A* **1965**, *140*, 1133−1138.

(28) Bauschlicher, C. W., Jr.; Ricca, A.; Partridge, H.; Langhoff, S. R. In *Recent Advances in Density Functional Methods, part II*; Chong, D. P., Ed.; World Scientific Publishing Company: Singapore, 1997; p 165.

(29) Lee, C.; Yang, W.; Parr, R. G. *Phys. Rev. B* **1988**, *37*, 785−789.

(30) Becke, A. D. *Phys. Rev. A* **1988**, *38*, 3098−3100.

(31) (a) Becke, A. D. *J. Chem. Phys.* **1993**, *98*, 1372−1377. (b) Becke, A. D. *J. Chem. Phys.* **1993**, *98*, 5648−5652.

(32) Stephens, P. J.; Devlin, F. J.; Chabalowski, C. F.; Frisch, M. J. *J. Phys. Chem.* **1994**, *98*, 11623−11627.

(33) Frisch, M. J.; et al. *Gaussian 03* Gaussian Inc.: Pittsburgh, PA, 2003. See Supporting Information for the complete citation.

(34) Schrödinger, L. L. C. *Jaguar*, 5.5; Portland, OR, 1991−2003.

(35) Siegbahn, P. E. M.; Blomberg, M. R. A. *Chem. Rev.* **2000**, *100*, 421−438.

(36) Siegbahn, P. E. M. *J. Comput. Chem.* **2001**, *22*, 1634−1645.

(37) Himo, F.; Siegbahn, P. E. M. *Chem. Rev.* **2003**, *103*, 2421−2456.

(38) Blomberg, M. R. A.; Siegbahn, P. E. M. *J. Phys. Chem. B* **2001**, *105*, 9375−9386.

(39) Pelmenschikov, V.; Blomberg, M. R. A.; Siegbahn, P. E. M. *J. Biol. Inorg. Chem.* **2001**, *7*, 284−298.

(40) Davydov, R.; Ledbetter-Rogers, A.; Martásek, P.; Larukhin, M.; Sono, M.; Dawson, J. H.; Masters, B. S. S.; Hoffman, B. M. *Biochemistry* **2002**, *41*, 10375−10381.

(41) Pufahl, R. A.; Wishnok, J. S.; Marletta, M. A. *Biochemistry* **1995**, *34*, 1930−1941.

(42) Dunford, H. B. In *Peroxidases in Chemistry and Biology*; Everse, J., Everse, K. E., Grisham, M. B., Eds.; CRC Press: Boca Raton, FL, 1991; Vol. 2, pp 1−24.

(43) Wirstam, M.; Blomberg, M.; Siegbahn, P. E. M. *J. Am. Chem. Soc.* **1999**, *121*, 10178−10185.

(44) Woon, D. E.; Loew, G. H. *J. Phys. Chem. A* **1998**, *102*, 10380−10384.

(45) Blomberg, M. R. A.; Siegbahn, P. E. M.; Babcock, G. T. *J. Am. Chem. Soc.* **1998**, *120*, 8812−8824.

(46) Wei, C. C.; Wang, Z. Q.; Durra, D.; Hemann, C.; Hille, R.; Garcin, E. D.; Getzoff, E. D.; Stuehr, D. J. *J. Biol. Chem.* **2005**, *280*, 8929−8935.

(47) Stuehr, D. J.; Cho, H. J.; Kwon, N. S.; Weise, M. F.; Nathan, C. F. *Proc. Natl. Acad. Sci. U.S.A.* **1991**, *88*, 7773−7777.